Pharmaceutical Sciences, 2022, 28(4), 552-563
doi:10.34172/PS.2022.6
https://ps.tbzmed.ac.ir/

Research Article

Synergistic Effect of Quercetin and Cobalt Ferrite-Graphene Oxide-Based Hyperthermia to Inhibit Expression of Heat Shock Proteins and Induce Apoptosis in Breast Cancer Cells

Fatemeh Mobaraki[1], Hojjatollah Nazari[2], Seyed Ali Lajevardiyan[3], Shadie Hatamie[4], Hanieh Jafary[1], Simzar Hosseinzadeh[5,6*]

[1]*Department of Biology, Science and Research Branch, Islamic Azad University, Tehran, Iran.*
[2]*Research Center of Advanced Technologies in Cardiovascular Medicine, Tehran Heart Center, Tehran University of Medical Sciences, Tehran, Iran.*
[3]*Department of Biochemistry, Faculty of Biological Science, North Tehran Branch, Islamic Azad University, Tehran, Iran.*
[4]*College of Medicine, National Taiwan University, 10048, Taipei, Taiwan.*
[5]*Medical Nanotechnology and Tissue Engineering Research Center, Shahid Beheshti University of Medical Sciences, Tehran, Iran.*
[6]*Department of Tissue engineering and Applied Cell Sciences, School of Advanced Technologies in Medicine, Shahid Beheshti University of Medical Sciences, Tehran, Iran.*

Article Info

Article History:
Received: 31 July 2021
Accepted: 28 January 2022
ePublished: 8 February 2022

Keywords:
-Breast cancer
-Heat shock proteins
-Hyperthermia
-Magnetic nanoparticles
-Quercetin

Abstract

Background: Combinatorial medicine includes promising therapeutic methods for diseases such as cancer, whereby various biochemical and physical agents are simultaneously used to remove tumors. For example, the effectiveness of hyperthermia as a new technique for cancer therapy, can be enhanced, if it is combined with chemical compounds. Herein, the influence of quercetin as a heat shock protein (HSP) inhibitor on the efficiency of cobalt ferrite-graphene oxide ($CoFe_2O_4$-GO) nanoparticles-based hyperthermia was investigated in an *in vitro* study.

Methods: Firstly, the surface of graphene sheets was decorated with $CoFe_2O_4$ nanoparticles (5-8 nm) and assayed using transmission electron microscopy (TEM), vibrating-sample magnetometer (VSM) and X-ray diffraction (XRD) methods. The cytotoxic effect of the corresponding co-implementation was then examined in MCF7 cell line with or without hyperthermia by (3-(4,5-dimethyl thiazolyl-2)-2,5-diphenyltetrazolium bromide) (MTT) test for 24, 48 and 72 hrs. In addition, the expression of *Bax*, *Bcl2* and *HSP70* genes and the production of radicals were evaluated by Real-Time PCR and DPPH (2,2-diphenyl-1-picrylhydrazyl) assays, respectively.

Results: The study showed that the doses associated with the IC_{50} points for quercetin and the $CoFe_2O_4$-GO nanocomposite were 0.02 mg/ml and 0.001 g/ml, respectively. The results showed that the simultaneous treatment of the cancer cells with quercetin, the nanocomposite, and hyperthermia significantly improves the cytotoxicity effect, increases the expression of *Bax* gene and down-regulates *HSP70* and *Bcl2* genes. In addition, the greatest attenuation of DPPH free radicals was observed in the corresponding group.

Conclusion: The hybrid treatment of quercetin and the nanoparticle in the presence of hyperthermia could be considered as a promising approach for cancer therapy with minor side effects.

Introduction

Breast cancer is one of the second most common types of cancer in the world. According to the World Health Organization (WHO), the incidence of these cancers has increased by about half a percent every year in last decade.[1] Unfortunately, standard cancer therapy methods used in clinics to treat patients, such as surgery, chemotherapy, radiation therapy, hormone therapy and targeted therapy, cannot completely cure cancer and sometimes, patients have serious side effects and relapses. Therefore, advanced interdisciplinary therapeutic methods such as nanotechnology and magnetic-based hyperthermia can be considered necessary for cancer research and therapy. For instance, there is an ongoing need to provide oncologists with chemoprophylactic formulizations to reduce or eliminate the side effects of conventional methods. The combination of hyperthermia-based methods with natural herbal components may serve as

*Corresponding Author: Simzar Hosseinzadeh, E-mail: s.hosseinzadeh@sbmu.ac.ir
©2022 The Author(s). This is an open access article and applies the Creative Commons Attribution Non-Commercial License (http://creativecommons.org/licenses/by-nc/4.0/). Non-commercial uses of the work are permitted, provided the original work is properly cited.

a better choice to be studied as influencing anti-cancer factors.[2] The introduction of certain plant extracts such as quercetin to induce apoptosis in various cancer cells as a therapeutic method has received too much attention worldwide.[3] Quercetin (3,3′,4′,5,7-pentahydroxyflavone) is an essential flavonoid in a diet.[4] This compound is found in many foods such as apples, onions, green tea, and nutritional supplements.[5] The biological and pharmacological properties of quercetin have anti-fibrotic, anti-atherogenic, anti-inflammatory, anti-allergic, anti-viral, anti-bacterial, anti-coagulant, anti-mutagenic and anti-cancer properties.[3,6] This flavonoid has been shown to inhibit the synthesis of heat shock proteins (HSPs) in cancer cells.[7] The heat shock response is a highly restrained molecular stress condition that induces the expression of stress proteins (HSPs) to preserve cells against high temperatures and a variety of stressful situations. Environmental, pathological and physiological stimuli induce significant increases in intracellular HSPs synthesis.[8] The major HSPs, including HSP 70, interact with components of the apoptotic pathway and induce cell survival by inhibiting mitochondrial outer membrane permeability and cytochrome C release. As a result, caspase activation and apoptosis are stopped.[9] Higher expression of HSPs protects against apoptosis in malignant neoplasms and treatment-induced apoptosis, which likely underlie the role of HSPs in tumor progression and resistance to treatment.[10] Besides, HSP expression levels are increased in various types of cancers, which leads to resistance to treatment and ultimately reducing patient life expectancy.[11,12] Therefore, neutralizing HSPs can be considered as an attractive strategy for the treatment of cancers. Medical nanotechnology has rapidly advanced and expanded over the past decade, leading to the research and development of different nanomaterials with enormous therapeutic potential.[13] For example, superparamagnetic nanoparticles (NPs) are able to have many potential applications in color imaging, magnetic cooling, biological fluids, controlled cancer drug delivery, magnetic resonance imaging (MRI), and hyperthermia to kill cancer cells by generating heat.[14-16] Magnetic NPs are able to react to time-dependent field changes and enable the transfer of energy from the exciting field to NPs. This advantage explains why NPs can cause an increase in temperature, since this property is used in hyperthermia to treat or intensify chemotherapy and radiation therapy.[17] Among magnetic NPs, cobalt ferrite $CoFe_2O_4$ NPs have attracted a great deal of attention due to their potentially diverse applications in industry and biomedicine fields. $CoFe_2O_4$ NPs show promise in biomedical applications such as drug delivery, magnetic heat, hyperthermia, biosensors, and magnetic resonance imaging.[18] Magnetic NPs have several benefits in treating tumors with hyperthermia. The performance of NPs for biomedical applications is often employed due to their narrow size distribution, suitable magnetic saturation, and low toxicity effects. Based on the large surface area of graphene oxide (GO) and its ability to form a stable colloidal suspension, many nanomaterials can be used to functionalize GO[19] and it has been shown that GO generally does not have vigorous cytotoxicity in general and is known to be a fairly safe material.[20] Hyperthermia is a promising treatment for the non-invasive or minimally invasive treatment of tumors alone or as a supplement to increase the effectiveness of chemotherapy and radiotherapy. In this method, NPs are injected into the cancerous mass and placed in an alternating magnetic field, which causes cancer cells to heat up to 41°C and ultimately destroy them. In a variable magnetic field, magnetic NPs generate heat, which leads to cell death of tumor cells. The process of magnetic damping involves the physical rotation of the particle (Brownian effect) or the movement of the magnetic moment without moving the particle (Neil effect).[21] This thermal stimulation activates the mechanisms of necrosis and cell death in neoplastic cells.[22] These particles can respond resonantly to time-dependent magnetic field changes and enable the transfer of energy from the excited field to the NPs.[23] The corresponding elevated temperature is used in hyperthermia for cancer treatment or as an enhancer of chemotherapy and radiotherapy.[17] In this study, we tried to inhibit HSP70 as one of the most important types of heat shock proteins in various cancers, through magnetic nanocomposites and quercetin. However, the complicated intracellular responses to NPs, the degree of cytotoxicity, and the mechanisms of their toxicity also depend on the method of preparation, the NPs components, the size, charge, and the charge and the target cell type.[24]

In the present study, due to the inhibitory role of quercetin on HSPs, it was used to improve hyperthermia-induced apoptosis by the nanoparticles in MCF7 cell line. Therefore, for first time, the viability, gene expression and radical formation of these cells were examined and compared between different experimental groups in order to find out the effect of this compound on hyperthermia.

Materials and Methods

Experimental reagents

Quercetin and polyvinyl pyrrolidone (PVP) were purchased from Sigma and the chemical materials including dimethyl sulfoxide (DMSO), cobalt chloride, ammonium solution, iron nitrate and methanol were provided from Merck. Also, Dulbecco's Modified Eagle's Medium DMEM (High Glucose), phosphate buffer saline (PBS), fetal bovine serum (FBS) and trypsin-EDTA were bought from Bio-idea. Moreover, 3-(4, 5-dimethylthiazol-2-yl)-2, 5-diphenyltetrazolium bromide (MTT) powder and Taq DNA polymerase enzyme were obtained from Sigma and Cina Gene respectively. TRIzol reagent for the RNA extraction and agarose for the electrophoresis process were taken respectively from Sigma and Sinaclon. Also, Amplicon supplied the enzyme Maxima SYBR Green qPCR Master Mix 2x, was used in the Real-time PCR technique. To measure the radical scavenging capacity of the nanoparticles, 2,2-diphenyl-1-picryl-hydrazyl-hydrate

(DPPH) was provided from Sigma.

Synthesis and characterization of $CoFe_2O_4$-GO nanocomposite

According to the manufacturing instruction of the above nanocomposite,[25,26] with short modifications and taking into account the molecular weight of each material, approximately 0.47 g of cobalt chloride per 10 ml of distilled water, 0.1 g of graphene oxide per 20 ml of distilled water, 1.6 g of nitrate iron per 10 ml of distilled water and 0.2 g of PVP per 30 ml of distilled water were weighed out. Each of the mentioned materials was stirred separately for 2-3 hrs. Then, all solutions were mixed and stored for 2 hrs to achieve a homogenous solution. After that, its pH was adjusted to 11-14 by using 25% ammonium solution. Then, the solution was poured into a metal container (reactor) and the lid was hermetically sealed and placed in an oven with the temperature of 180 ° C for 3 hrs. After cooling, the contents were transferred into a beaker and allowed to settle on the bottom. The final material was washed several times with distilled water and its supernatant was discarded. In order to use the nanocomposite for cell treatments, it was mixed with PBS (100 mg/ml) and dispersed by means of an ultrasonic homogenizer. Prior to the experiment, the NPs dispersion in PBS was diluted with cell culture medium to a final concentration of 60, 30, 10, 8, 4, 2, and 1 mg/ml. In order to investigate the size, morphology, and decoration of the graphene sheets with $CoFe_2O_4$ NPs, the nanocomposite was fixed on carbon grids and examined with a transmission electron microscope (TEM, PHILIPS 30 with the acceleration voltage of 250 kV). Also, the prepared nanoparticles were examined using the vibrating-sample magnetometer (VSM) method (VSM-7300, Meghnatis Daghigh Kavir Co., Kashan, Iran). The test was performed at room temperature and a maximum applied field of 10 kOe. The resulting curves were evaluated to find out the magnetic activity of the nanoparticles. Moreover, the composite nanoparticles were examined by X-ray diffraction (XRD) technique. This assessment was carried out with an X-ray diffraction device, Philips, PW 1730. The radiation source was CuKα radiation with an applied voltage of 35 kV. The assay was conducted at room temperature and the wavelength of the radiation was 1.5418 Å.

Cell culture

Human breast adenocarcinoma MCF7 cell line was purchased from National Center for Genetic and Biological Resources of Iran) and they were cultured in DMEM supplemented with FBS (10%), l-glutamine (2 mM), and antibiotics (penicillin 100 units/µl; streptomycin 100 µg/µl). The cells were incubated at 37°C in a humidified atmosphere 5% CO_2 until they reached 80% confluence.

Cell viability

MTT assay was used to compare the effect of quercetin and the $CoFe_2O_4$-GO nanocomposite, with and without the hyperthermia process on cell viability. Briefly, MCF7 cells (5×10^3 cells / well) were seeded in 96-well plates. The cells were incubated for 24 hrs at 37°C and 5% CO2 in high glucose DMEM medium containing 10% FBS. The $CoFe_2O_4$-GO nanocomposite (60, 30, 10, 8, 4, 2 and 1 mg/ml) and quercetin (0, 1, 2, 3, 5, 8, 10 and 15 µg/ml) were added to the cells separately. It should be noted that the concentrations of quercetin and the $CoFe_2O_4$-GO nanocomposite were equal to their IC_{50} points, when they were used simultaneously to evaluate their synergistic effect as a combination condition. The cell viability assessments were carried out after 24, 48 and 72 hrs. For this assay, the MTT solution (0.1%) was added to the cells and after 3 hrs, the developed formazan crystals were dissolved in DMSO and their absorbance was read at 570 nm. The cell viability values were calculated accordance with below formula:

Cell viability (%) = ODt / ODc × 100

Where OD is abbreviation of optical density and ODt determines the absorbance of a treated group and ODc is the representative of the non-treated group (control group).

Thermal activation of $CoFe_2O_4$-GO nanocomposite

Radio frequency (RF) absorption of NPs is assessed by measuring their temperature after insertion in a magnetic field. This temperature defines the amount of heat generated per unit mass of a magnetic NP per unit time. For this evaluation, a hyperthermia research system (LAB A, HT-1000W, NATSYCO) with a frequency range of 100 to 400 kHz was used to apply an alternating magnetic field to the nanocomposite solution. One ml of a nanocomposite suspension at a specific concentration, was poured to a glass tube and inserted into the water-cooled magnetic induction coil of the hyperthermia system. The temperature was monitored with a digital thermometer. The concentration ranges of the nanocomposite that could increase the temperature above 45°C, was selected for the cell treatments.

Cellular hyperthermia test

The cell line of MCF7 was incubated in culture media and treated with the selected groups including quercetin + nanoparticles + hyperthermia and cells + quercetin + nanoparticles + hyperthermia. The IC_{50} points of the NPs and quercetin were employed to treat the cells in this assessment. After that, the copper coil of a hyperthermia research system was located in the treated cell samples and the magnetic field with the following values was applied. The frequency and power with the respective values of 300 kHz and 1000 W for 15 min were considered as the optimal hyperthermia parameter amounts on MCF7 cell line. These optimized values were obtained by monitoring the temperature of the corresponding concentrations (IC_{50} points) in various frequency and power levels and eventually, the values that raised the temperature to 45°C, were considered the optimal values (data not shown). The MTT assay was carried out for 24, 48 and 72 hrs.

RNA extraction and quality control of extracted RNA

MCF7 cells were seeded at a density of (5×10^3 cells/well) in 96-well plates. After that, $CoFe_2O_4$-GO nanocomposite and quercetin were added to the wells at their optimized concentrations. The hyperthermia process was applied and after 72 hrs, the RNA of the cells was extracted. The cell groups were divided into the groups that were treated with the nanocomposite, quercetin, and a combination of both quercetin and the nanocomposite. However, the non-treated cells was considered as the control group to calibrate the corresponding test groups. The total RNA was extracted with TRIzol reagent and the quality of the RNA extraction was detected by subjecting 5 µl of the RNA to a 1.5% agarose gel during the electrophoresis process. The bands and their strength indicated the extractability and health of the desired RNA. To determine the contamination of the RNA samples with proteins, 2 µl of the extracted products was diluted by adding 98 µl of RNase-DNase free water and its absorbance was measured at 260 and 280 nm.

cDNA synthesis from total RNA and Real-Time PCR assay

The total RNA of the test and control cell groups was use to prepare cDNA using the Random Hexamer primer and reverse transcriptase (M-MuLV RT). For the synthesis of each cDNA, 1 µg of the purified RNA was mixed with 1 µl of the Random Hexamer primer. The volume of the batch was increased to 10 µl with RNase-DNase free water and as shown in Table 1, the samples were placed in a thermal cycler at a temperature of 75°C for 5 minutes. In order to ensure the optimal concentration of cDNA for Real-Time PCR assay, PCR procedure was performed. In this reaction, 1 and 0.5 µl of the cDNAs were processed in accordance with Table 2. After that, Real-Time PCR was carried out to detect the expression of *HSP70*, *Bax* and *BcL2* genes. The primer sequences of these genes is listed in Table 3. Furthermore, the HPRT1 gene was selected as a reference gene in order to normalize the expression of the marker genes. The volume of each component of the reaction samples are collected in Table 4. Finally, the Real-Time PCR reaction schedule and the associated melt program were respectively done according to Tables 5 and 6. The

Table 1. Primer sequences of target and internal control genes for Real-Time PCR.

Gene	Sequences from 5' to 3'	Annealing temperature
HPRT1-F	CCTGGCGTCGTGATTAGTG	60°C
HPRT1-R	TCAGTCCTGTCCATAATTAG TCC	60°C
H-Bax-F	CAAACTGGTGCTCAAGGC	60°C
H-Bax-R	CACAAAGATGGTCACGGTC	60°C
H-Bcl2-F	GATAACGGAGGCTGGGATG	62°C
H-Bcl2-R	CAGGAGAAATCAAACAGA GGC	62°C
HSP70-F	GCTATTATGGCAGATAGACA GAG	59°C
HSP70-R	TGTTACGATCTTCACTCAC	59°C

Table 2. Temperature condition of cDNA synthesis reaction temperature.

Time	Temperature
10 min	25°C
15 min	37°C
45 min	42°C (Optimal temperature of enzyme activity)
10 min	75°C (To inactivate the enzyme)

Table 3. PCR reaction program for cDNA synthesis.

Number of cycles	Time	Temperature	Stage
1	7 s	95°C	Enzyme activation
35	30 s	95°C	Denaturation
	30 s	60°C	Annealing
	30 s	72°C	Extention
1	7 s	72°C	Final Extention

QIAGEN Rotor-Gene Q (Corbett Rotor-Gene 6000) was used for the Real-Time PCR assay. All PCRs were carried out in a total volume of 25 µl, with 12.5 µl of SYBRGreen PCR Master Mix, 5 µl of the cDNAs (300 ng), 1 µl of the primers (0.5 µl of the forward primer and 0.5 µl of the reverse primer) and 6.5 µl of double-distilled water.

Radical scavenging activity of CoFe2O4-GO nanoparticles

The free radical scavenging activity of quercetin, nanoparticles, quercetin + nanoparticles and quercetin

Table 4. Reagents of Real-Time PCR.

Components	Volume (µl)
SYBR Green Master Mix qPCR 2X high Rox (Amplicon)	6.5
Forward Primer (10 pmol)	0.5
Reverse Primer (10 pmol)	0.5
Template (cDNA)	1
ddH_2O	4.5

Table 5. Conditions of denature and PCR cycling in Real-Time PCR.

Cycle	Time	Temperature	Stages
1	15 min	95°C	Enzyme activation
40	15 min	95°C	Denaturation
	1 min	60°C	Annealing and Extension

Fluorescence emission reading by the device was done at the end of the elongation phase in the FAM/SYBR channel.

Table 6. Melting conditions in Real-Time PCR.

Time	Temperature	Stages
2 s	95°C	1
60 s	60°C	2
50 s	95°C	3
1 s	0.3 °C	Rate

+ nanoparticles + hyperthermia was examined by DPPH method. In addition, the assay was repeated for these treatment groups in the presence of MCF7 cells. For this analysis, the cells were treated with quercetin, nanoparticles, quercetin + nanoparticles and quercetin + nanoparticles + hyperthermia and after 72 hrs, 2 ml of the DPPH solution was added at a concentration of 0.016 g per 20 ml of methanol. The reaction was completed after 30 min at room temperature and the absorbance of the samples were read at 520 nm. The radical inhibition percentage was calculated using the following formula:

Inhibition percentage = $(A_{blank}-A_{sample})/A_{blank} \times 100$

Where A_{blank} and A_{sample} are the absorption rates of the control (DPPH solution) and the samples at 520 nm, respectively.

Statistical analysis

In order to indicate the significant differences between the control and test groups in all assays, t-test student method was employed, but the normality of the data was essential to initiate the corresponding analysis. In this regard, when the *p-values* were greater than 0.5, the relationship was reported as significant relation. While, if the value was less or equal to 0.5, it was considered insignificant. All results were reported in the present study as mean ± standard deviation (SD).

Results

Characterization of $CoFe_2O_4$-GO nanocomposite

Morphology, shape, size, and decoration of the $CoFe_2O_4$ NPs on graphene sheets were examined under high magnification with a TEM device. Microscopic images showed that the $CoFe_2O_4$ NPs with a mean size of 5-8 nm were decorated with a fine dispersion on the surface of graphene nanosheets (Figure 1a-c). In addition, the hyperthermia machine that was used for the hyperthermia process, is clear in Figure 1d. Also, in order to evaluate the magnetic properties of the nanocomposite, VSM assay was done and shown in Figure 2a. The maximum applied field was 15 kOe at room temperature and the magnetic saturation of the nanocomposite was about 30 emu/g. The nanocomposite coercivity was diminished indicating that the corresponding cobalt ferrite NPs exhibited superparamagnetic behavior. As reported before, the magnetic NPs can be superparamagnetic when their size is below than the critical value of about 6-8 nm.[27] Another characterization assay of the composite nanoparticles was XRD. According to Figure 2b, the corresponding XRD pattern confirmed several peaks between 10-80º. A broad diffraction peak at 2θ of ~ 19º is representative of the residual graphite components during the graphene oxide synthesis. Also, the graphene oxide films developed another peak at 23º.[28] The plane of this peak is (002) which was replaced due to the interactions between the graphene oxide sheets and the magnetic nanoparticles from 21º[29] to

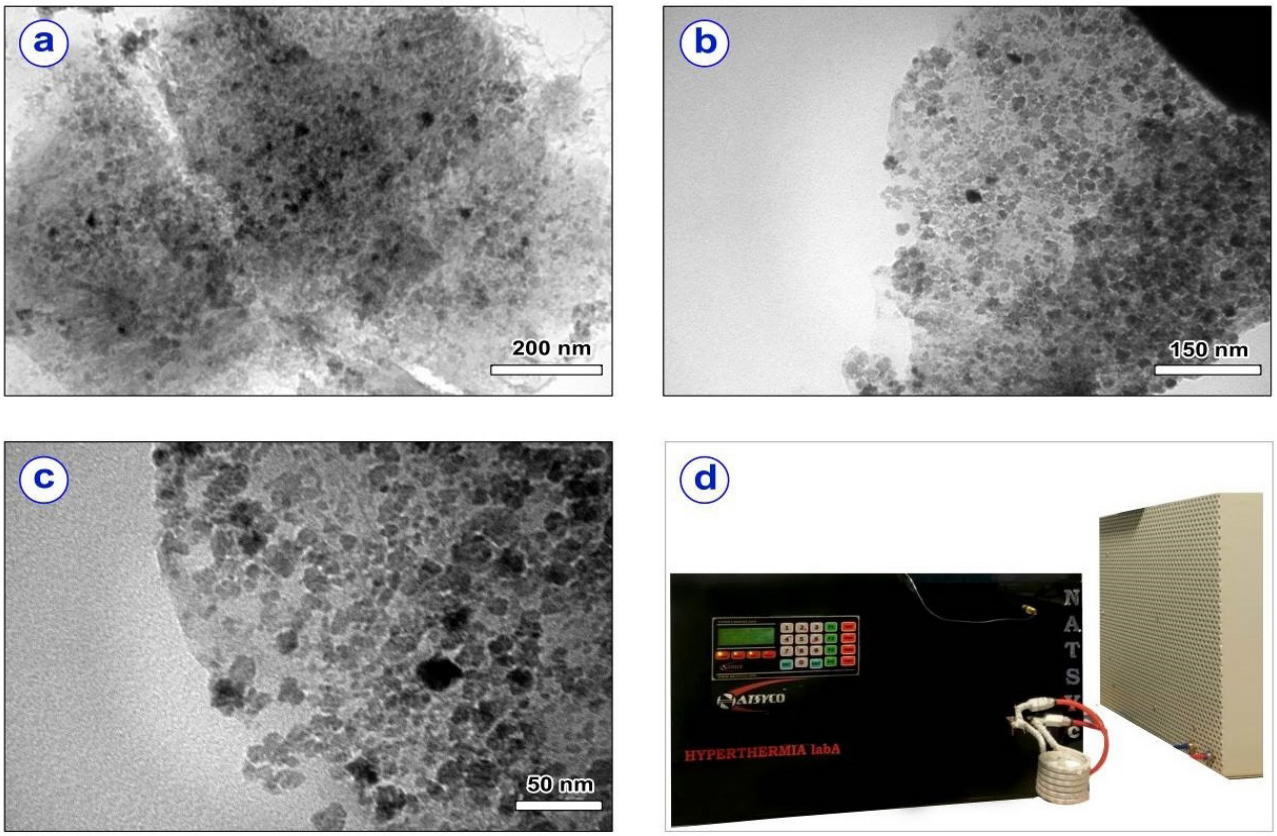

Figure 1. TEM micrograph of $CoFe_2O_4$-GO nanocomposite at the scale of a) 200 nm, b)150 nm, c) 50 nm and d) the hyperthermia machine which was employed to the assessments.

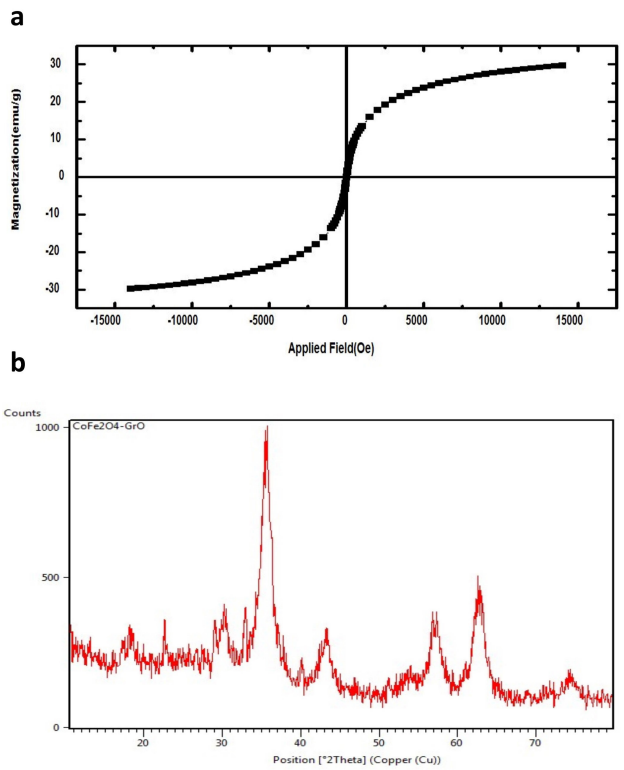

Figure 2. VSM diagram a) and XRD pattern b) of $CoFe_2O_4$-GO nanocomposite.

23°. On the other hand, the 2θ peaks at 30, 36, 43.5, 57.2 and 63° are associated to the cobalt ferrite nanoparticles. The plane of these peaks are respectively (220), (311), (400), (511) and (440).[17] As a whole, this assay approved that the cobalt ferrite nanoparticles created a cubic spinel structure on the graphene oxide sheets.

Cell morphology and viability

The cytotoxic effect of different concentrations of quercetin and the $CoFe_2O_4$-GO magnetic nanocomposite, with or without the action of magnetic field via hyperthermia, was investigated with MTT test at different times (24, 48, and 72 hrs). The toxic effects of quercetin are necessary to induce apoptosis of MCF7, therefore the IC_{50} point is calculated for the following tests. The IC_{50} concentration was determined to be 2 µM after 72 hrs (Figure 3a). On the other hand, the first results showed that after treating cancer cells with different concentrations of $CoFe_2O_4$-GO nanocomposite (0.01, 0.03, and 0.06 g/ml), a very high percentage of cells died, and the OD level of all groups was decreased to zero (Figure 3b). Therefore, the effect of nanocomposite diluent concentrations was examined, and the dose including the half-maximal toxicity (IC_{50}) was observed at a concentration of 0.001 g/ml (Figure 3c). Next, it was shown that cancer cells treated with both magnetic nanocomposite and hyperthermia at the optimal concentration of 0.001 g/ml at intervals of 24, 48, and 72, respectively, significantly increased the lethality of hyperthermia (Figure 3d). After obtaining effective concentrations of quercetin and the $CoFe_2O_4$-GO nanocomposite in the lethal range of IC_{50}

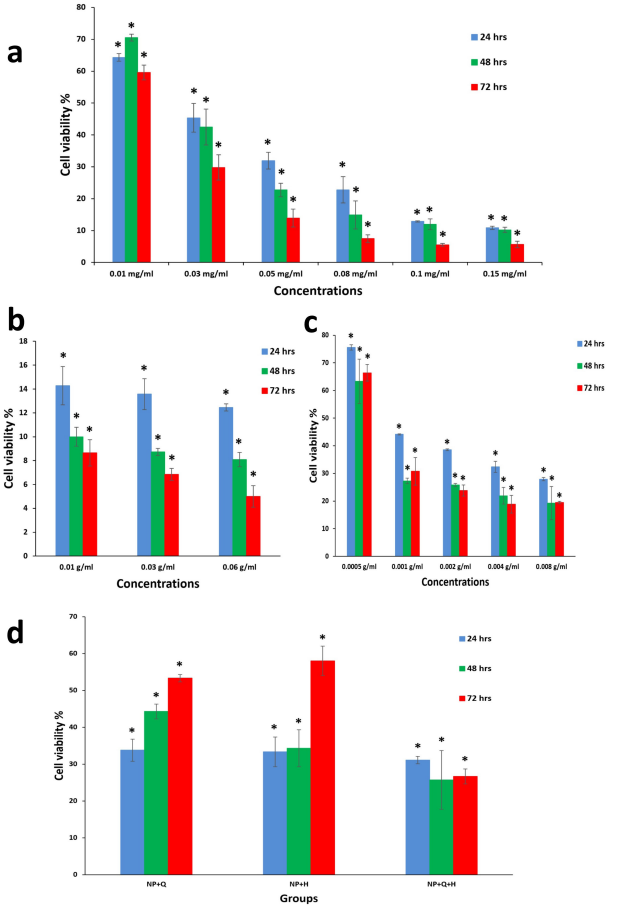

Figure 3. MTT test results in MCF7 cell line after their treatments with a) quercetin, b) $CoFe_2O_4$-GO nanocomposite at the concentrations of 0.01, 0.03 and 0.06 g/ml, c) $CoFe_2O_4$-GO nanocomposite at the concentrations of 0.01, 0.03 and 0.06 g/ml, d) 0.0005, 0.001, 0.002, 0.004 and 0.008 g/ml and d) combination groups of $CoFe_2O_4$-GO nanocomposite/quercetin (NP+Q), $CoFe_2O_4$-GO nanocomposite/hyperthermia (NP+H) and $CoFe_2O_4$-GO nanocomposite/quercetin/hyperthermia (NP+Q+H). The asterisks indicate the significant relationships between the treated cell groups and the non-treated cell group (p-value < 0.05).

($CoFe_2O_4$-GO nanocomposite: 0.001 g/ml, quercetin: 0.02 mg/ml), the possibility of the synergistic effect of these factors on the viability of MCF7 cells was evaluated in the presence and absence of hyperthermia was assessed. The results showed that the OD of the cells decreased more than four-fold in the presence of hyperthermia, and a higher lethality was observed with the combined method (Figure 3). Micrographs of MCF7 cells treated with quercetin, $CoFe_2O_4$-GO nanocomposite, hyperthermia/$CoFe_2O_4$-GO nanocomposite, and hyperthermia/$CoFe_2O_4$-GO nanocomposite/quercetin demonstrated their abilities on cell death (Figure 4a-d). As shown in Figure 4, the cell mortality increased after the combination of hyperthermia and quercetin, which was confirmed by MTT tests.

Real-time PCR

Real-time PCR was used to evaluate changes in the expression of the genes including *Bcl2* and *Bax* (*HSP70*) genes in MCF7 cells treated with quercetin,

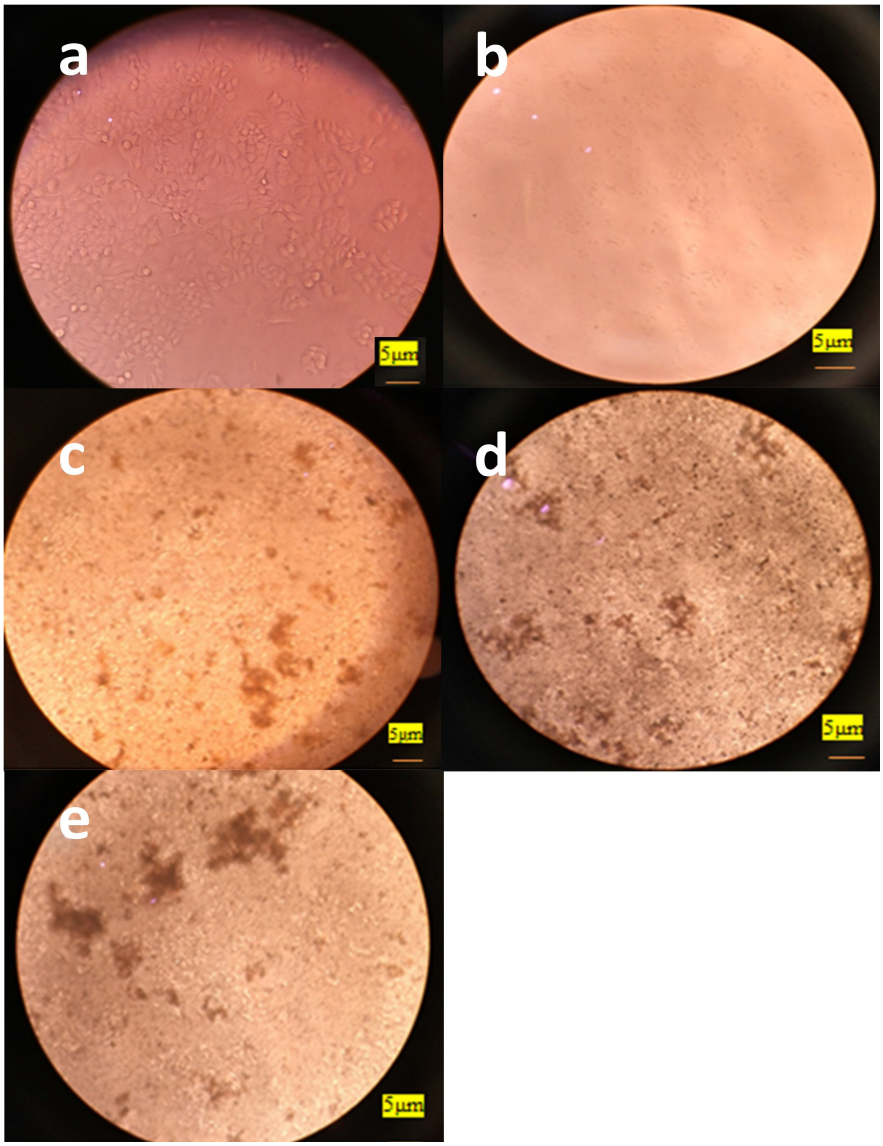

Figure 4. Optical microscopic images of a) non-treated MCF7 cells and treated MCF7 cells with b) Quercetin, c) $CoFe_2O_4$-GO nanocomposite, d) $CoFe_2O_4$-GO nanocomposite/hyperthermia and e) $CoFe_2O_4$-GO nanocomposite/hyperthermia/Quercetin after 72 hours. (Scale bar: 5 µm).

$CoFe_2O_4$-GO nanocomposite, hyperthermia/$CoFe_2O_4$-GO nanocomposite and hyperthermia/$CoFe_2O_4$-GO nanocomposite/quercetin after 72 hrs. Agarose gel electrophoresis confirmed the cDNA fabrication process for real-time PCR (Figure 5a). The results showed that the genes *Bax*, *Bcl2*, and *HSP70* genes showed the highest expression when the cells were treated with quercetin or hyperthermia/$CoFe_2O_4$-GO nanocomposite/quercetin or hyperthermia/$CoFe_2O_4$-GO nanocomposite (Figure 5b). Regarding to the *Bax* gene, after the treatment of MCF7 cells with the three corresponding factors, its expression increased. Besides, the expression of the *Bcl2* gene illustrated an increasing mode in all groups except the group of $CoFe_2O_4$-GO nanocomposite. The expression of the *HSP70* gene was also increased in the groups treated with the nanocomposite and hyperthermia/ nanocomposite.

DPPH assay

The DPPH (2,2-diphenyl-1-picrylhydrazyl) assay was employed to assess the anti-oxidant activity of quercetin and $CoFe_2O_4$-GO nanocomposite. The results indicated that both $CoFe_2O_4$-GO nanocomposite and quercetin had more significant free radicals than the DPPH solution. However, there were no significant differences in anti-oxidant activity between quercetin and $CoFe_2O_4$-GO nanocomposite (Figure 6a). Next, the effect of the DPPH solution on MCF7 cells treated with quercetin, $CoFe_2O_4$-GO nanocomposite, hyperthermia/$CoFe_2O_4$-GO nanocomposite, and hyperthermia/$CoFe_2O_4$-GO nanocomposite/quercetin was examined. As shown in Figure 6b, the anti-oxidant properties were significantly increased by treating cancer cells with quercetin in different groups. However, the treatment of the cells with $CoFe_2O_4$ led to the fact that the GO nanoparticles enhance the radical production by the cells even in the absent of

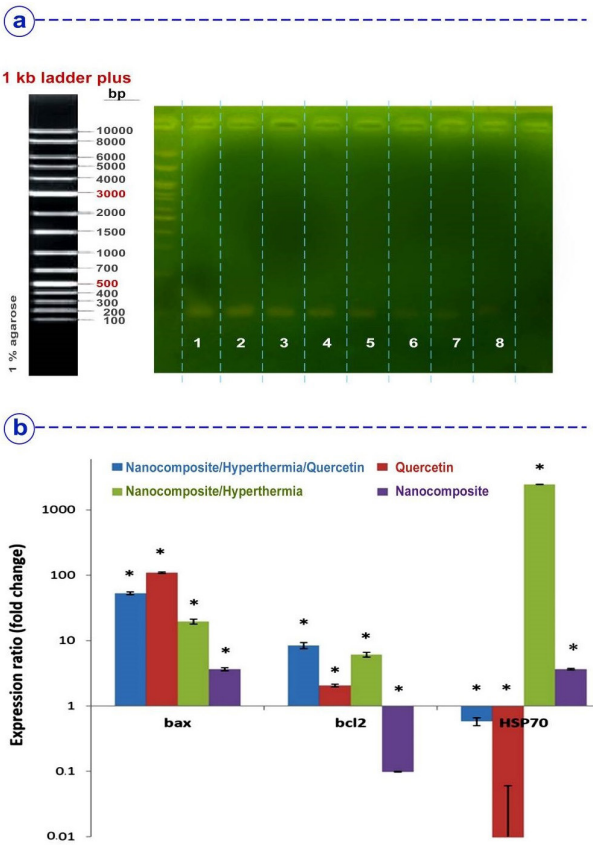

Figure 5. a) Agarose gel electrophoresis of cDNA obtained treated MCF7 cells after 72 hrs (1, 2, 3 and 4 correspond to 1 µL of the cDNAs obtained from the treated MCF7 cell line with quercetin, $CoFe_2O_4$-GO nanocomposite, $CoFe_2O_4$-GO nanocomposite/quercetin and $CoFe_2O_4$-GO nanocomposite/quercetin/hyperthermia respectively. Besides, 6, 7 and 8 correspond to 0.5 µL of the cDNAs obtained from the treated MCF7 cell line with quercetin, $CoFe_2O_4$-GO nanocomposite, $CoFe_2O_4$-GO nanocomposite/quercetin and $CoFe_2O_4$-GO nanocomposite/quercetin/hyperthermia respectively), b) The expression levels of Bax, bcl2 and HSP70 genes in MCF7 cell line after their treatments with quercetin, $CoFe_2O_4$-GO nanocomposite, $CoFe_2O_4$-GO nanocomposite/quercetin, and $CoFe_2O_4$-GO nanocomposite/quercetin/hyperthermia after 72 hrs. The asterisks indicate the significant relationships between the treated cell groups and the non-treated cell group (p-value < 0.05).

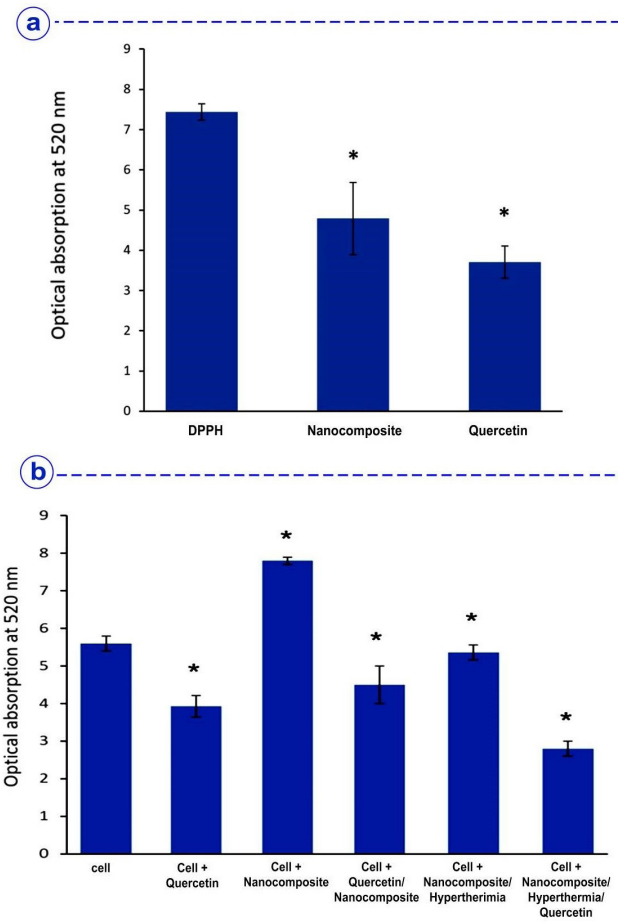

Figure 6. a) Free radical attenuation of DPPH solution, $CoFe_2O_4$-GO nanocomposite and quercetin (The asterisks indicate the significant relationships between the groups and DPPH solution (p-value < 0.05)), b) Free radical attenuation of the non-treated MCF7 cell line, the treated with quercetin, $CoFe_2O_4$-GO nanocomposite, quercetin/$CoFe_2O_4$-GO nanocomposite, $CoFe_2O_4$-GO nanocomposite/hyperthermia and quercetin/$CoFe_2O_4$-GO nanocomposite/hyperthermia (The asterisks indicate the significant relationships between the treated cell groups and the non-treated cell group (p-value < 0.05).

hyperthermia. It is shown that the simultaneous use of hyperthermia and the nanoparticles could reduce the radical property of the nanocomposite. The results also showed that the highest level of anti-oxidants is occurred when the cells are treated with hyperthermia/$CoFe_2O_4$-GO nanocomposite/quercetin.

Discussion

Combination therapy methods are now considered as effective options in the treatment of various cancer types, including breast cancers. For example, they combine molecular-based therapy methods with biophysical concepts such as hyperthermia approaches, based on the implementation of magnetic fields and heat generation in cancer cells and tissues. This strategy can be seen as an effective tool in the treatment of breast cancer. However, the development of the efficiency of hyperthermia, which is considered to be one of the most promising advanced methods in cancer treatment, depends on the emergence and development of safe and highly efficient magnetic nanostructures. On the other hand, some drugs that intervene in this area, particularly those that inhibit heat shock proteins, may increase the induction of apoptosis in cancer cells through molecular and cellular pathways. This study reports for the first time a combination therapy consisting of the simultaneous use of a heat shock protein inhibitor called quercetin and hyperthermia based on $CoFe_2O_4$-GO nanocomposite, albeit in the form of an *in vitro* study. $CoFe_2O_4$ magnetic nanoparticles are biocompatible reagents with inverted spinel structures from the mixed metal oxides category. Thus, they have received a lot of attention in the treatment of cancers in recent years.[30] However, the accumulation of these nanoparticles in nanostructured layers such as graphene oxide and molybdenum disulfide can increase their efficiency in

hyperthermia due to the intensification of the oscillation and the generation of thermal energy in an external magnetic field. On the other hand, the binding of these NPs to the surface of graphene sheets, can reduce their potential toxicity and agglomeration during *in vivo* and *in vitro* studies. In a recent study, Wang *et al.*[31] covered the surface of graphene sheets with $CoFe_2O_4$ NPs (with a diameter of 5-13 nm) for theranostic purposes, diagnosis of cancer by MRI and chemotherapy. These applications resulted in increased cancer cell death and better image quality. In another study, Mallick *et al.*[32] decorated the surface of graphene sheets with zink-substituted lithium ferrite NPs and developed a new nanocomposite that increases the efficiency of hyperthermia for cancer therapy.[32] In another study by our team, the surface of molybdenum disulfide nanosheets was decorated with $CoFe_2O_4$ NPs (with a diameter of 17 ± 4 nm) for hyperthermia purposes.[33] In this study, accordance with TEM nanographs, the $CoFe_2O_4$ NPs with a diameter of 5-8 nm are successfully distributed on the surface of graphene nanosheets. Accordance with before studies, the nanoparticles up to 10 nm in diameter indicate a superparamagnetic property and can generate heat via Néel relaxation.[34] On the other hand, superparamagnetic NPs have attracted attention for cancer treatment because of their easy control and local heat generation and in particular, these nanoparticles inhibit overheating of healthy cells.[35] Herein, after the production and morphological /chemical confirmations of the $CoFe_2O_4$-GO nanocomposite, its combination therapy based on quercetin and hyperthermia was evaluated *in vitro*. Initially, after 72 hrs, the MTT test results showed that the IC_{50} (concentration required to prevent 50% of cancer cell proliferation) for quercetin and $CoFe_2O_4$-GO nanocomposite are 0.02 mg/ml and 0.001 g/ml, respectively. Furthermore, the treatment of cancer cells with quercetin/$CoFe_2O_4$-GO nanocomposite for 72 hrs decreased the OD value of the cells by 1.9 times. Besides, the addition of the hyperthermia field reduced the OD by 3.7 times demonstrating the prominent role of the hyperthermia in this combination therapy. In the next step, we evaluated the effect of a hyperthermia-based combination therapy with quercetin and the $CoFe_2O_4$-GO nanocomposite on the expression of HSPs and apoptosis-related genes. HPSs are the sum of the proteins expressed in the cells under stress and due to various environmental, pathological and physiological conditions, they play a crucial role in preventing conformational changes in proteins under stress factors and apoptosis.[9] HSPs protect cells from various types of cytotoxic stimulators.[20] With regard to cancer therapy, the increased expression of HSPs protects cancer cells from the induction and initiation of apoptosis.[36,37] This problem explains the negative and disruptive role of HSPs in reducing the effectiveness of treatment, leading to tumor progression and resistance to therapy. In this context, we also investigated the extent of changes in the expression of the *HSP70* gene under the influence of quercetin, a so-called HSP inhibitor. HSP70 is a heat shock protein that inhibits apoptosis by interacting with Apoptosis-Inducing Factor (AIF) or Apoptotic protease activating factor 1 (Apaf1) via inhibiting Jun N-terminal Kinase (JNK) and Bcl-2-associated X protein (Bax) mitochondrial displacement.[38-40] This molecule also inhibits apoptosis by protecting the essential core proteins of the caspase-3 cleavage and concerns the molecules such as F-actin, BH3-interacting domain (Bid) and reactive oxygen species (ROS).[41,42] Our study found that the simultaneous treatment of MCF7 cells with the $CoFe_2O_4$-GO nanocomposite and quercetin under hyperthermal conditions, decreased the expression of HSP70. However, more down-regulation was observed, when the cells were treated with quercetin alone. Similarly, Hosokawa *et al.*[43] also observed that the down-regulating effect of quercetin on HSP70 protein expression is more significant at normal temperature (37°C). In addition, Clarke and colleagues showed that the HSP70 family is involved in repairing defective proteins and preventing apoptosis induction. Therefore, the reduced expression of this gene can lead to apoptosis of cancer cells.[41] Surprisingly, the treatment of the cells with the $CoFe_2O_4$-GO nanocomposite and hyperthermia increased the level of *HSP70* gene. Examination of changes in the expression of genes involved in apoptosis, including *Bcl2* and *Bax*, also demonstrated the apoptotic effectiveness of our proposed combination method. For example, *Bcl2* is well-known as an apoptosis inhibitor and maintains the integrity of the mitochondrial membrane and prevents the release of cytochrome C.[44] On the other hand, Bax family proteins are apoptosis inducers that trigger apoptosis through their incorporation into the mitochondrial membrane and the stimulation cytochrome C.[45,46] In addition, the expression of *Bax* gene is upregulated in all study groups, but, the largest increase is associated with the quercetin-treated group.

With regard to *Bcl2* down-regulation, only treatment of the cancer cells with the $CoFe_2O_4$-GO nanocomposite decreased the expression of this gene and other groups showed a slight positive regulation of this gene. Also, the group treated with quercetin and the nanoparticle in the presence of hyperthermia process, showed greater expression of the apoptosis-related gene; *Bax*. Quercetin has also received a lot of attention as a potential anti-cancer agent and numerous studies have described its cancer prophylactic properties and anti-genotoxic effects.[47,48] The anti-cancer properties of quercetin are attributed to its anti-oxidant activity, inhibiting cancer-causing activating enzymes, modulating signaling pathways and interacting with receptors and other proteins involved in cell division.[49-51] With regard to the oxidation capacity of the elements, the studies on the DPPH radical scavenging activity showed that the $CoFe_2O_4$-GO nanocomposite and quercetin release a significant amount of anti-oxidants. Besides, the DPPH assay have also shown that the treatment of MCF7 cells with the $CoFe_2O_4$-GO nanocomposite without implementing hyperthermia, surprisingly induces free radical release. On the contrary, the presence of

quercetin in each treatment group leads to anti-oxidant properties, which are most often observed in the hybrid group in the presence of hyperthermia.

Conclusion

In this study, the surface of graphene oxide nanosheets has been decorated by the $CoFe_2O_4$ NPs, leading to the fabrication of a magnetic nanocomposite for hyperthermia. Then, MCF7 cells were treated with different concentrations of quercetin, the $CoFe_2O_4$-GO nanocomposite, and their mixture with and without implementing a magnetic field for hyperthermia. The *in vitro* gene and viability study showed that the incubation of MCF7 cell line with quercetin for 72 hrs is able to increase apoptosis, inhibit proliferation, decrease their survival, and significantly downregulate *HSP70* gene expression at 37.5°C. Furthermore; also it has been observed that the effect of the magnetic $CoFe_2O_4$-GO nanocomposite along with hyperthermia induces apoptosis in MCF7 cancer cells through induction of *Bax* gene expression. Finally, the simultaneous treatment of cancer cells with quercetin, the $CoFe_2O_4$-GO nanocomposite, and hyperthermia decreases the expression of the *HSP70* gene due to the effect of heat shock compared to quercetin. However, this method decreased *Bcl2* gene expression and increased Bax gene expression. Moreover, the hybrid method can be considered as a therapeutic method with minor damages to natural cells, because of the high anti-oxidant potential of quercetin.

Acknowledgments

The authors declare that they have no known competing financial interests or personal relationships that could have influenced the work reported in this paper. The corresponding research was done using the grant (ID: 18244) and the ethical number of IR.SBMU.RETECH.REC.1398.378 from Shahid Beheshti University of Medical Sciences.

Author Contributions

Study concept, data analysis and revision: SH, laboratory assays: FM and SAL, drafting of manuscript: HN, nanoparticle synthesis: SH and data analysis: HJ.

Conflict of Interest

The authors report no conflicts of interest.

References

1. DeSantis CE, Ma J, Gaudet MM, Newman LA, Miller KD, Goding Sauer A, et al. Breast cancer statistics, 2019. CA: Cancer J Clin. 2019;69:438-51. doi:10.3322/caac.21583
2. Sharma G, Park J, Sharma AR, Jung J-S, Kim H, Chakraborty C, et al. Methoxy poly (ethylene glycol)-poly (lactide) nanoparticles encapsulating quercetin act as an effective anticancer agent by inducing apoptosis in breast cancer. Pharm Res. 2015;32:723-35. doi:10.1007/s11095-014-1504-2
3. De Whalley CV, Rankin SM, Hoult JRS, Jessup W, Leake DS. Flavonoids inhibit the oxidative modification of low density lipoproteins by macrophages. Biochem Pharmacol. 1990;39:1743-50. doi:10.1016/0006-2952(90)90120-A
4. Heim KE, Tagliaferro AR, Bobilya DJ. Flavonoid antioxidants: chemistry, metabolism and structure-activity relationships. J Nutr Biochem. 2002;13:572-84. doi:10.1016/S0955-2863(02)00208-5
5. Havsteen B. Flavonoids, a class of natural products of high pharmacological potency. Biochem Pharmacol. 1983;32:1141-8. doi:10.1016/0006-2952(83)90262-9
6. Perez-Vizcaino F, Bishop-Bailley D, Lodi F, Duarte J, Cogolludo A, Moreno L, et al. The flavonoid quercetin induces apoptosis and inhibits JNK activation in intimal vascular smooth muscle cells. Biochem. Biophys. Res. Commun. 2006;346:919-25. doi:10.1016/j.bbrc.2006.05.198
7. Kudo M, Naito Z, Yokoyama M, Asano G. Effects of quercetin and sunphenon on responses of cancer cells to heat shock damage. Exp Mol Pathol. 1999;66:66-75. doi:10.1006/exmp.1999.2247
8. Georgopoulos C, Welch W. Role of the major heat shock proteins as molecular chaperones. Annu Rev Cell Biol. 1993;9:601-34. doi:10.1146/annurev.cb.09.110193.003125
9. Beere HM. Death versus survival: functional interaction between the apoptotic and stress-inducible heat shock protein pathways. J Clin Invest. 2005;115:2633-9. doi:10.1172/JCI26471
10. Arrigo A-P, Paul C, Ducasse C, Manero F, Kretz-Remy C, Virot S, et al. Small stress proteins: novel negative modulators of apoptosis induced independently of reactive oxygen species. Prog Mol Subcell Biol. 2002;28:185-204. doi:10.1007/978-3-642-56348-5_10
11. Van't Veer LJ, Dai H, Van De Vijver MJ, He YD, Hart AA, Mao M, et al. Expression profiling predicts clinical outcome of breast cancer. Breast Cancer Res. 2003;5:57. doi:10.1186/bcr562
12. Ciocca DR, Calderwood SK. Heat shock proteins in cancer: diagnostic, prognostic, predictive, and treatment implications. Cell Stress Chaperones. 2005;10:86. doi:10.1379/CSC-99r.1
13. Magaye R, Zhao J, Bowman L, Ding M. Genotoxicity and carcinogenicity of cobalt-, nickel-and copper-based nanoparticles. Exp Ther Med. 2012; 4: 551-61. doi:10.3892/etm.2012.656
14. Yamaura M, Fungaro DA. Synthesis and characterization of magnetic adsorbent prepared by magnetite nanoparticles and zeolite from coal fly ash. J Mater Sci. 2013;48:5093-101. doi:10.1007/s10853-013-7297-6
15. Lu W, Shen Y, Xie A, Zhang W. Green synthesis and characterization of superparamagnetic Fe3O4 nanoparticles. J Magn Magn Mater. 2010;322:1828-33. doi:10.1016/j.jmmm.2009.12.035
16. Moon J-W, Roh Y, Lauf RJ, Vali H, Yeary LW, Phelps TJ.

Microbial preparation of metal-substituted magnetite nanoparticles. J Microbiol Methods. 2007;70:150-8. doi:10.1016/j.mimet.2007.04.012
17. Hatamie S, Balasi ZM, Ahadian MM, Mortezazadeh T, Shams F, Hosseinzadeh S. Hyperthermia of breast cancer tumor using graphene oxide-cobalt ferrite magnetic nanoparticles in mice. J Drug Deliv Sci Technol. 2021;65:102680. doi:10.1016/j.jddst.2021.102680
18. Farzaneh S, Hosseinzadeh S, Samanipour R, Hatamie S, Ranjbari J, Khojasteh A. Fabrication and characterization of cobalt ferrite magnetic hydrogel combined with static magnetic field as a potential bio-composite for bone tissue engineering. J Drug Deliv Sci Technol. 2021;64:102525. doi:10.1016/j.jddst.2021.102525
19. Liu H, Xi P, Xie G, Shi Y, Hou F, Huang L, et al. Simultaneous reduction and surface functionalization of graphene oxide for hydroxyapatite mineralization. J Phys Chem C. 2012;116:3334-41. doi:10.1021/jp2102226
20. Chang Y, Yang S-T, Liu J-H, Dong E, Wang Y, Cao A, et al. In vitro toxicity evaluation of graphene oxide on A549 cells. Toxicol Lett. 2011;200:201-10. doi:10.1016/j.toxlet.2010.11.016
21. Huang HS, Hainfeld JF. Intravenous magnetic nanoparticle cancer hyperthermia. Int J Nanomedicine. 2013;8:2521. doi:10.2147/IJN.S43770
22. Gupta AK, Gupta M. Synthesis and surface engineering of iron oxide nanoparticles for biomedical applications. Biomaterials. 2005;26:3995-4021. doi:10.1016/j.biomaterials.2004.10.012
23. Esmaeili E, Soleimani M, Ghiass MA, Hatamie S, Vakilian S, Zomorrod MS, et al. Magnetoelectric nanocomposite scaffold for high yield differentiation of mesenchymal stem cells to neural-like cells. J Cell Physiol. 2019;234:13617-28. doi:10.1002/jcp.28040
24. Sohaebuddin SK, Thevenot PT, Baker D, Eaton JW, Tang L. Nanomaterial cytotoxicity is composition, size, and cell type dependent. Part Fibre Toxicol. 2010;7:22. doi:10.1186/1743-8977-7-22
25. Wang G, Ma Y, Mu J, Zhang Z, Zhang X, Zhang L, et al. Monodisperse polyvinylpyrrolidone-coated CoFe2O4 nanoparticles: Synthesis, characterization and cytotoxicity study. Appl Surf Sci. 2016;365:114-9. doi:10.1016/j.apsusc.2016.01.031
26. Hatamie S, Ahadian MM, Ghiass MA, Saber R, Parseh B, Oghabian MA, et al. Graphene/cobalt nanocarrier for hyperthermia therapy and MRI diagnosis. Colloids Surf B. 2016;146:271-9. doi:10.1016/j.colsurfb.2016.06.018
27. Karaagac O, Bilir B, Kockar H. Superparamagnetic cobalt ferrite nanoparticles: effect of temperature and base concentration. J Supercond Nov Magn. 2015;28:1021-7. doi:10.1007/s10948-014-2798-3
28. Blanton TN, Majumdar D. Characterization of X-ray irradiated graphene oxide coatings using X-ray diffraction, X-ray photoelectron spectroscopy, and atomic force microscopy. Powder Diffr. 2013;28:68-71. doi:10.1017/S0885715613000109
29. Kim Y, Noh Y, Lim EJ, Lee S, Choi SM, Kim WB. Star-shaped Pd@ Pt core–shell catalysts supported on reduced graphene oxide with superior electrocatalytic performance. J Mater Chem A. 2014;2:6976-86. doi:10.1039/C4TA00070F
30. Cruz M, Ferreira L, Ramos J, Mendo S, Alves A, Godinho M, et al. Enhanced magnetic hyperthermia of CoFe2O4 and MnFe2O4 nanoparticles. J Alloys Compd. 2017;703:370-80. doi:10.1016/j.jallcom.2017.01.297
31. Wang G, Ma Y, Wei Z, Qi M. Development of multifunctional cobalt ferrite/graphene oxide nanocomposites for magnetic resonance imaging and controlled drug delivery. Chem Eng Sci. 2016;289:150-60. doi:10.1016/j.cej.2015.12.072
32. Mallick A, Mahapatra A, Mitra A, Greneche J-M, Ningthoujam R, Chakrabarti P. Magnetic properties and bio-medical applications in hyperthermia of lithium zinc ferrite nanoparticles integrated with reduced graphene oxide. Int J Appl Phys. 2018;123:055103. doi:10.1063/1.5009823
33. Alavijeh MS, Maghsoudpour A, Khayat M, Rad I, Hatamie S. Cobalt ferrite decoration of molybdenum disulfide nanosheets; development of a nanocomposite-mediated hyperthermia method. J Mech Sci Technol. 2021;35:1319-25. doi:10.1007/s12206-020-1242-9
34. Bakoglidis K, Simeonidis K, Sakellari D, Stefanou G, Angelakeris M. Size-dependent mechanisms in AC magnetic hyperthermia response of iron-oxide nanoparticles. IEEE Trans Magn. 2012;48:1320-3. doi:10.1109/TMAG.2011.2173474
35. Hedayatnasab Z, Abnisa F, Daud WMAW. Review on magnetic nanoparticles for magnetic nanofluid hyperthermia application. Mater Des. 2017;123:174-96. doi:10.1016/j.matdes.2017.03.036
36. Samali A, Cotter TG. Heat shock proteins increase resistance to apoptosis. Exp Cell Res. 1996;223:163-70. doi:10.1006/excr.1996.0070
37. Ikwegbue PC, Masamba P, Oyinloye BE, Kappo AP. Roles of heat shock proteins in apoptosis, oxidative stress, human inflammatory diseases, and cancer. Pharmaceuticals. 2018;11:2. doi:10.3390/ph11010002
38. Roufayel R, Kadry S. Molecular chaperone HSP70 and key regulators of apoptosis-a review. Curr Mol Med. 2019;19:315-25. doi:10.2174/1566524019666190326114720
39. Boudesco C, Cause S, Jego G, Garrido C. Hsp70: A cancer target inside and outside the cell. In: Calderwood S, Prince T. editors. Chaperones. Methods in Molecular Biology, vol 1709. Humana Press: New York, NY; 2018. doi:10.1007/978-1-4939-7477-1_27
40. Vostakolaei MA, Hatami-Baroogh L, Babaei G, Molavi O, Kordi S, Abdolalizadeh J. Hsp70 in cancer: A double agent in the battle between survival and death. J Cell Physiol. 2021;236: 3420-44. doi:10.1002/jcp.30132
41. Powers MV, Clarke PA, Workman P. Death by

chaperone: HSP90, HSP70 or both? Cell Cycle. 2009;8:518-26. doi:10.3892/ijo.2015.3213
42. Harahap N, Amelia R, Sibuea A, Manalu N, Novita N. HSP70 (heat shock protein 70) expression and antioxidant as a protective againts oxidative stress triggered by sub-maximal physical activity. IOP Conf Ser Earth Environ Sci. 2021; 713(1):012051. doi:10.1088/1755-1315/713/1/012051
43. Hosokawa N, Hirayoshi K, Nakai A, Hosokawa Y, Marui N, Yoshida M, et al. Flavonoids inhibit the expression of heat shock proteins. Cell Struct Funct. 1990;15:393-401. doi:10.1247/csf.15.393
44. Tzifi F, Economopoulou C, Gourgiotis D, Ardavanis A, Papageorgiou S, Scorilas A. The role of BCL2 family of apoptosis regulator proteins in acute and chronic leukemias. Adv Hematol. 2012;2012:524308. doi:10.1155/2012/524308
45. Pawlowski J, Kraft AS. Bax-induced apoptotic cell death. PNAS. 2000;97:529-31. doi:10.1073/pnas.97.2.529
46. Hosseinzadeh S, Nazari H, Esmaeili E, Hatamie S. Polyethylene glycol triggers the anti-cancer impact of curcumin nanoparticles in sw-1736 thyroid cancer cells. J Mater Sci Mater Med. 2021;32:112. doi:10.1007/s10856-021-06593-9
47. Rauf A, Imran M, Khan IA, ur-Rehman M, Gilani SA, Mehmood Z, et al. Anticancer potential of quercetin: A comprehensive review. Phytother Res. 2018;32:2109-30. doi:10.1002/ptr.6155
48. Davoodvandi A, Shabani Varkani M, Clark CC, Jafarnejad S. Quercetin as an anticancer agent: Focus on esophageal cancer. J Food Biochem. 2020;44:e13374. doi:10.1111/jfbc.13374
49. Mrkus L, Batinić J, Bjeliš N, Jakas A. Synthesis and biological evaluation of quercetin and resveratrol peptidyl derivatives as potential anticancer and antioxidant agents. Amino acids. 2019;51:319-29. doi:10.1111/bph.12409
50. Oliver S, Yee E, Kavallaris M, Vittorio O, Boyer C. Water soluble antioxidant dextran–quercetin conjugate with potential anticancer properties. Macromol Biosci. 2018;18(4):e1700239. doi:10.1002/mabi.201700239
51. Hashemzaei M, Delarami Far A, Yari A, Heravi RE, Tabrizian K, Taghdisi SM, et al. Anticancer and apoptosis-inducing effects of quercetin in vitro and in vivo. Oncol Rep. 2017;38:819-28. doi:10.3892/or.2017.5766